The Initiation, Propagation, and Effect of Matrix Microcracks in Cross-Ply and Related Laminates †

John A. Nairn, Shoufeng Hu, Siulie Liu, Jong Bark
Material Science and Engineering Department
University of Utah, Salt Lake City, Utah 84112

ABSTRACT

Recently, a variational mechanics approach has been used to determine the thermoelastic stress state in cracked, $[0_n/90_m]_s$ laminates (J. A. Nairn, *J. Comp. Mat.*, **23**, 1106 (1989)). This paper describes a generalization of the variational mechanics techniques to handle other cross-ply laminates ($[90_n/0_m]_s$), related laminates ($[\pm\theta/90_m]_s$, $[90_m/\pm\theta]_s$, *etc.*), and to account for delaminations emanating from microcrack tips. Microcracking experiments on Hercules 3501-6/AS4 carbon fiber/epoxy $[90_n/0_m]_s$ laminates show a staggered cracking pattern. These results can be explained by the variational mechanics analysis. The analysis of delaminations emanating from microcrack tips has resulted in predictions about the structural and material variables controlling competition between microcracking and delamination failure modes.

INTRODUCTION

Many observations have confirmed that the initiation of damage in multidirectional laminates is often by microcracks in the off-axis plies that run parallel to the fibers in those plies [1-8]. These microcracks have typically been studied in cross-ply laminates in which the cracks form in the 90° plies [1-8]. Microcracks form during static testing [1-8], during fatigue testing [3,9,10], and during thermal cycling [11]. Because microcracks cause a reduction in stiffness [3], a change in the thermal expansion coefficient [12,13], and provide sites for the initiation of delaminations, it is important to gain a quantitative understanding of the formation and propagation of microcracks. Two important factors that must be understood are

1. The formation of microcracks in 90° plies is dependent on laminate structure. That is, the cracking process depends on the thickness of the 90° layers, the support provided to the 90° layers by other plies, and whether the 90° plies are on the inside or are adjacent to a free edge.

2. The residual thermal stresses in the 90° plies of cross-ply laminates are typically tensile and of sufficient magnitude to influence the microcracking process.

STRESS ANALYSIS TECHNIQUES

Several attempts have been made at the stress analysis of cross-ply laminates using simplistic analyses (e.g. shear-lag analyses [2,4,6,7,14,15]). While these simplistic models often yield qualitatively reasonable results, they are unsuitable for a thorough understanding of microcracking. Hashin [16,17] was the first to apply variational mechanics techniques. He solved for the modulus [16,17] and the thermal expansion coefficient [18] of $[0_n/90_m]_s$ laminates as a function of microcrack density. Nairn *et al.* [19,20] have extended Hashin's analysis to include residual thermal stresses and to the fracture mechanics analysis of microcracking in $[0_n/90_m]_s$ laminates. This paper describes the variational mechanics approach, how it can be extended to more difficult problems involving $[90_n/0_m]_s$, $[\pm\theta/90_n]_s$, and $[90_n/\pm\theta]_s$ laminates, and how it can analyze delaminations emanating from microcrack tips. In this section, we outline the variational mechanics stress analysis techniques.

Consider a laminate plate with the x axis parallel to the zero degree fibers, the y axis parallel to the 90° fibers, and the z axis normal to the plane of the plate. When the 90° plies have through-the-width microcracks (as is invariably observed in static testing), a two-dimensional analysis of the x-z plane suffices. The x-z plane, or laminate edge, can conveniently be divided into multiple layers (n layers). The layers may

---

be assigned to individual plies, ply groups, or portions of a ply, depending on the nature of the problem being solved and on the desired accuracy. For the stress state within any layer, we make one and only one assumption — that the x-axis tensile stresses depend only on x and are independent of z. A general stress state for the ith layer that fulfills this assumption and equilibrium is [19,20]

$$\sigma_{xx}^{(i)} = \sigma_{x0}^{(i)} - \psi_i(\xi) \tag{1}$$

$$\sigma_{xz}^{(i)} = \lambda_i f_i(\xi, \zeta) \tag{2}$$

$$\sigma_{zz}^{(i)} = -\lambda_i^2 g_i(\xi, \zeta) \tag{3}$$

where superscript (i) denotes stress in the ith layer, $\sigma_{x0}^{(i)}$ is the x axis tensile in the uncracked laminate, $\lambda_i = t_i/t_*$, $\psi_i(\xi)$ is a function of the dimensionless x direction coordinate $\left(\xi = x/t_*\right)$, f_i and g_i are functions of ξ and of the dimensionless z direction coordinate $\left(\zeta = \left(z - z_0^{(i)}\right)/t_i\right)$, and $z_0^{(i)}$ is the z coordinate at the start of the ith layer. In these equations, t_i is the thickness of the ith layer and t_* is the thickness of any arbitrarily chosen normalization thickness. The functions f_i, g_i, and ψ_i are interrelated by

$$\frac{\partial f_i}{\partial \xi} = \frac{\partial g_i}{\partial \zeta} \tag{4}$$

$$\psi_i' = \frac{\partial \psi_i}{\partial \xi} = \frac{\partial f_i}{\partial \zeta} \tag{5}$$

We consider a unit cell of damage of a multilayered sample that extends from $x = a$ to $x = -a$ or from $\xi = \rho = a/t_*$ to $\xi = -\rho$. We further consider each layer to be orthotropic with at least one symmetry axis aligned with either the x or z axes. Generalizing the two-layer results from Ref. [19] to n layers, the total complementary energy in the unit cell of damage per unit depth (y direction dimension) can be written as

$$\Gamma = \Gamma_0 + t_*^2 \sum_{i=1}^{n} \int_{-\rho}^{\rho} \left[\frac{\lambda_i \psi_i^2}{2E_{xi}} - \frac{\nu_i \lambda_i^3 \psi_i}{E_{xi}} \int_0^1 g_i d\zeta + \frac{\lambda_i^5}{2E_{zi}} \int_0^1 g_i^2 d\zeta + \frac{\lambda_i^3}{2G_i} \int_0^1 f_i^2 d\zeta \right. $$
$$\left. + \lambda_i^3 \left(\frac{\sigma_{x0}^{(i)} \nu_i}{E_{xi}} - \alpha_{zi} \Delta T \right) \int_0^1 g_i d\zeta - \alpha_{xi} \lambda_i \Delta T \psi_i \right] d\xi \tag{6}$$

where E_{xi}, E_{zi}, G_i, ν_i, α_{xi}, and α_{zi} are the mechanical properties of the ith layer, being, respectively, x and z direction tensile moduli (E_{xx} and E_{zz}), in-plane shear modulus (G_{xz}), in-plane Poisson's ratio (ν_{xz}), and x and z direction thermal expansion coefficients. The term $\Delta T = T_0 - T_s$ is the temperature differential between the stress-free temperature (T_0) and the specimen temperature (T_s). The term Γ_0 is a constant energy term that does not enter energy minimization procedures.

The analysis procedure for a large variety of problems are similar:

1. From observation of experimental results, model microcracking damage by a unit cell of damage extending from $x = -a$ to $x = a$.

2. Divide the laminate into n layers where the divisions are chosen for sufficient accuracy.

3. Using boundary conditions and stress continuity conditions, express the f_i and g_i functions in terms of the ψ_i functions and explicit functions of ζ (this step is always possible).

4. Rewrite the total complementary energy in integral form involving only the ψ_i functions.

5. Using the calculus of variations, minimize the complementary energy to solve for the ψ_i functions. The principals of variational mechanics state that these functions will provide the best approximation to the true stress state.

6. With knowledge of the ψ_i functions, it is possible to find the sample modulus [16,17,19], the thermal expansion coefficient [18,19], the total strain energy [19,20], and the energy release rate due to the propagation of damage [19,20].

When n is large, solving for all the ψ_i functions will necessarily involve numerical calculations. The solution of such problems can be viewed as a complementary energy based finite element (or layer) analysis. When n is small ($n \leq 4$), however, it is often possible to eliminate all but one or two of the ψ_i functions. In such situations, the resulting calculus of variations problem can be solved in closed form. Fortunately, many interesting and relevant cross-ply laminate problems can be expressed with four or fewer layers. The remainder of this paper outlines the solutions to some of these problems.

MICROCRACKING IN $[0_n/90_m]_s$ LAMINATES

When loaded in tension, $[0_n/90_m]_s$ laminates fail in a nearly periodic array of through-the-width microcracks in the 90° plies. The unit cell of damage is shown in Fig. 1A. Because the problem is symmetric about the midplane, the laminate can be divided into two layers of thicknesses t_1 and t_2 (see Fig. 1A). Layer 1 is half the 90° ply group and layer 2 is one of the 0° ply groups. We need to solve for ψ_1 and ψ_2, one of which can be eliminated by force balance. As shown in Ref. [19], the total complementary energy in the unit cell of damage per unit depth can be written in terms of ψ_1 as

$$\Gamma = \Gamma_0 + t_1^2 \int_{-\rho}^{\rho} \left[C_1 \psi_1^2 + C_2 \psi_1 \psi_1'' + C_3 \psi_1''^2 + C_4 \psi_1'^2 - 2\Delta\alpha\Delta T \psi_1 \right] d\xi \tag{7}$$

where $\Delta\alpha = \alpha_T - \alpha_A$, and

$$C_1 = \frac{1}{E_T} + \frac{1}{\lambda E_A} \qquad\qquad C_2 = \frac{\nu_T}{E_T}\left(\lambda + \frac{2}{3}\right) - \frac{\lambda\nu_A}{3E_A}$$
$$C_3 = \frac{1}{60E_T}(15\lambda^2 + 20\lambda + 8) + \frac{\lambda^3}{20E_T} \qquad C_4 = \frac{1}{3G_T} + \frac{\lambda}{3G_A} \tag{8}$$

Here, E, G, ν and α denote tensile and shear moduli, Poisson's ratio, and thermal expansion coefficient, subscripts A and T denote axial and transverse properties of the ply material, and $\lambda = t_2/t_1$.

Minimization of the complementary energy in Eq. (7) has been accomplished in Ref. [19]. We quote some useful results. Consider a sample with N unit cells of damage characterized by crack spacings $\rho_1, \rho_2, \ldots, \rho_N$. The sample compliance is [16,19]

$$C = C_0 + \frac{2t_1 C_3 L E_T^2}{B^2 W E_c^2} \frac{\sum_{i=1}^{N} \chi(\rho_i)}{\sum_{i=1}^{N} \rho_i} \tag{9}$$

where W is the sample width (y-direction dimension), L is the sample length (x-direction dimension), E_c is the modulus of the uncracked sample, and $C_0 = L/BE_cW$ is the compliance of the uncracked sample. The new function $\chi(\rho)$ has a physical interpretation as being proportional to the excess strain energy caused by the presence of the microcracks. Defining $p = (C_2 - C_4)/C_3$, $q = C_1/C_3$,

$$\chi(\rho) = 2\alpha\beta\left(\alpha^2 + \beta^2\right)\frac{\cosh 2\alpha\rho - \cos 2\beta\rho}{\beta\cosh 2\alpha\rho + \alpha\sin 2\beta\rho} \qquad \text{for } \frac{4q}{p^2} > 1 \tag{10}$$

$$\chi(\rho) = \alpha\beta(\beta^2 - \alpha^2)\frac{\tanh\beta\rho\tanh\alpha\rho}{\beta\tanh\beta\rho - \alpha\tanh\alpha\rho} \qquad \text{for } \frac{4q}{p^2} < 1 \tag{11}$$

where for $4q/p^2 > 1$

$$\alpha = \frac{1}{2}\sqrt{2\sqrt{q} - p} \qquad \text{and} \qquad \beta = \frac{1}{2}\sqrt{2\sqrt{q} + p} \tag{12}$$

and for $4q/p^2 < 1$

$$\alpha = \sqrt{-\frac{p}{2} + \sqrt{\frac{p^2}{4} - q}} \qquad \text{and} \qquad \beta = \sqrt{-\frac{p}{2} - \sqrt{\frac{p^2}{4} - q}} \tag{13}$$

We note that the expression for sample compliance (Eq. (9)) has no adjustable parameters and is applicable to any distribution of crack spacings (not just periodic arrays of cracks). Hashin [16] has shown that this expression is in excellent agreement with experimental data.

Table I: The critical microcracking fracture toughness, G_{mc}, for five different carbon fiber composite material systems. Details of experiments given in Ref. [20].

Prepreg Material	G_{mc} (J/m^2)
Hercules 3501-6/AS4	240
Fiberite 934/T300	690
DuPont Avimid® K Polymer/IM6	960
Fiberite 977-2/T300	1800–2400
ICI PEEK/AS4	3000

The total strain energy in the N crack intervals can be written as [19]

$$U = \left(\frac{\sigma_0^2}{2E_c} + \frac{t_1 \Delta \alpha^2 \Delta T^2}{BC_1} \right) BWL + (C - C_0)\frac{B^2 W^2 E_c^2}{2E_T^2} \left(\frac{E_T^2}{E_c^2}\sigma_0^2 - \frac{\Delta \alpha^2 \Delta T^2}{C_1^2} \right) \tag{14}$$

where σ_0 is the total stress applied to the laminate. The longitudinal thermal expansion coefficient of the cracked sample is [19,20]

$$\alpha_L = \alpha_L^0 - \frac{C - C_0}{C_0} \frac{\Delta \alpha}{C_1 E_T} \tag{15}$$

where α_L^0 is the longitudinal thermal expansion coefficient of the uncracked sample. Finally, combining all expressions, we can derive an expression for the energy release rate due to the formation of additional microcracks [19,20]

$$G_m = \left(\frac{E_T}{E_c}\sigma_0 - \frac{\Delta \alpha \Delta T}{C_1} \right)^2 C_3 t_1 \frac{d}{dD}(D\langle \chi(\rho) \rangle) \tag{16}$$

where $\langle \chi(\rho) \rangle$ is the average value of $\chi(\rho)$ over the N crack spacings and $D = \frac{N}{L}$ is the crack density. We note that Eq. (16) is slightly different than the result from Ref. [19] and corrects an error in that paper. The correct result is derived in Ref. [20].

If we assume that the formation of microcracks is governed by a critical energy release rate or a microcracking fracture toughness, G_{mc}, we can use Eq. (16) to predict the initiation and the increase in crack density in $[0_n/90_m]_s$ laminates. To use Eq. (16), we must evaluate the density derivative of $D\langle \chi(\rho) \rangle$. The formation of a new microcrack between two existing microcracks is shown in Fig. 1B; the crack is shown to form in the middle because that is the location of the maximum stress and because of the tendency of these laminates towards periodic crack spacings. By a discrete evaluation of the required derivative

$$G_m = \left(\frac{E_T}{E_c}\sigma_0 - \frac{\Delta \alpha \Delta T}{C_1} \right)^2 C_3 t_1 (2\chi(\rho/2) - \chi(\rho)) \tag{17}$$

Given a value of the fracture toughness of a material system, G_{mc}, we can solve Eq. (17) for applied stress, σ_0, and predict the crack density as a function of applied stress. This approach was applied in Ref. [20] to five material systems; for each material system, two to five cross-ply laminates were used. Some typical results for Hercules 3501-6/AS4 carbon fiber/epoxy laminates are given in Fig. 2. For this material, G_{mc} was found to be 240 J/m². An important result for this and other materials systems is that a single value of G_{mc} for a given material system suffices to predict the results from all cross-ply laminates tested. Some measured values of G_{mc} are given in Table I.

The variational mechanics analysis of microcracked $[0_n/90_m]_s$ laminates has been useful. Without any adjustable parameters it gives an excellent prediction of the sample modulus as a function of crack density [16]. When implemented into a fracture mechanics analysis of microcracking, it can predict the crack density as a function of applied load [19,20]. Combining experimental results and the energy release rate expression in Eq. (17), it is possible to measure G_{mc}. G_{mc} appears to be a useful material parameter characterizing microcracking or *intralaminar* fracture toughness of composite materials.

MICROCRACKING IN $[90_n/0_m]_s$ LAMINATES

The damage process in $[90_n/0_m]_s$ laminates is more complicated than in $[0_n/90_m]_s$ laminates. When $[90_n/0_m]_s$ laminates are loaded in tension, the 90° plies on either side develop nearly periodic arrays of through-the-width microcracks. Comparing the crack patterns on either side, however, we observe that the cracks on one side are shifted by half a crack spacing from the cracks on the opposite side. Thus, any given microcrack is located approximately midway between two microcracks on the opposing surface. The unit cell of damage for such "staggered" microcracks is shown in Fig. 3A. Because the problem is no longer symmetric about the midplane, we must analyze the entire laminate; we thus divide the laminate into four layers according the ply groups (see Fig. 3A). Layers 1 and 4 are 90° ply groups and layers 2 and 3 divide the 0° ply group into two layers. We need to solve for ψ_1 to ψ_4, two of which can be eliminated by force balance and transverse stress free-edge effects. Finding the complementary energy for this system is a much more difficult than for the $[0_n/90_m]_s$ laminates. The details will be described in a future publication. In this paper we give the key results. The total complementary energy in the unit cell of damage per unit depth in terms of ψ_1 and ψ_4 is

$$\Gamma = \Gamma_0 + t_1^2 \int_0^{\frac{\xi}{2}} \left(C_1 X^2 + C_{2a} X X'' + C_{3a} X''^2 + C_4 X'^2 - 4\Delta\alpha\Delta T X \right.$$
$$\left. + C_1^* Y^2 + C_2^* Y Y'' + C_3^* Y''^2 + C_4^* Y'^2 \right) d\xi \tag{18}$$

where $X = \psi_1 + \psi_4$, $Y = \psi_1 - \psi_4$, C_1 and C_4 are given in Eq. (8), and the new constants are

$$C_{2a} = -\frac{\nu_T}{3E_T} + \frac{\nu_A}{E_A}\left(1 + \frac{2\lambda}{3}\right) \qquad C_{3a} = \frac{1}{20E_T} + \frac{\lambda}{60E_T}\left(8\lambda^2 + 20\lambda + 15\right)$$

$$C_1^* = \frac{1}{E_T} + \frac{(1+2\lambda)^2}{\lambda^3 E_A} \qquad C_2^* = -\frac{\nu_T}{3E_T} + \frac{\nu_A}{E_A}\left[\frac{(1+2\lambda)(2+\lambda)}{3\lambda}\right] \tag{19}$$

$$C_3^* = \frac{1}{20E_T} + \frac{\lambda}{60E_T}\left(2\lambda^2 + 7\lambda + 8\right) \qquad C_4^* = \frac{1}{3G_T} + \frac{1+\lambda+\lambda^2}{3\lambda G_A}$$

Minimizing the complementary energy in Eq. (18) would be an intractable problem if it were not for the following symmetry relation between ψ_1 and ψ_4:

$$\psi_4(\xi) = \begin{cases} \psi_1(\xi - \rho) & \text{for } \xi > 0 \\ \psi_1(\xi + \rho) & \text{for } \xi < 0 \end{cases} \tag{20}$$

With this relation, it is possible to minimize the complementary energy in closed form. The details (which are more complicated than the $[0_n/90_m]_s$ problem) will be described in a future publication.

Because the stress analysis of $[90_n/0_m]_s$ laminates is a new solution, we begin with a brief discussion of the resulting stresses. The tensile stress $\sigma_{xx}^{(1)}$, or the tensile stress in the 90° ply on the left of Fig. 3A is plotted in Fig. 4; the plot is for a Hercules 3501-6/AS4 carbon fiber/epoxy $[90_2/0]_s$ laminate with a crack spacing characterized by $\rho = 3$. At the two crack faces $\sigma_{xx}^{(1)} = 0$ as required by boundary conditions. Midway between the two microcracks and directly opposite the crack in the 90° ply on the opposing surface (see Fig. 3A) there is a local minimum in tensile stress. This local minimum is caused by a bending effect that results from the asymmetric arrangement of microcracks. Two local maxima in stresses are located near $\rho = \pm 1$ or at positions roughly $\frac{1}{3}$ and $\frac{2}{3}$ of the way from the bottom microcrack to the top microcrack. The form of the stresses in Fig. 4 can be used to explain the tendency towards staggered microcracks. In Fig. 3B, we show new microcracks formed at all local stress maxima. It is observed that the new microcrack pattern is equivalent to three unit cells of damage and thus the distribution of the stresses naturally leads to the propagation of staggered microcracks.

We next quote some useful results of the new $[90_n/0_m]_s$ laminate analysis. It is possible the cast these results in a form that is reminiscent of the $[0_n/90_m]_s$ laminate results. Consider a sample with N unit cells of damage characterized by crack spacings $\rho_1, \rho_2, \ldots, \rho_N$. The sample compliance is

$$C = C_0 + \frac{2t_1 C_{3a} L E_T^2}{B^2 W E_c^2} \frac{\sum_{i=1}^N \chi_a(\rho_i)}{\sum_{i=1}^N \rho_i} \tag{21}$$

501

$C \cdot 2$

where the new function $\chi_a(\rho)$ has a physical interpretation as being proportional to the excess strain energy caused by the presence of the microcracks; it is defined by

$$\chi_a(\rho) = \frac{2\chi\left(\frac{\ell}{2}\right)}{1 + \frac{C_{3a}\chi\left(\frac{\ell}{2}\right)}{C_3^*\chi^*\left(\frac{\ell}{2}\right)}} \tag{22}$$

In Eq. (22), $\chi(\rho)$ is defined by Eq. (11), except that C_{2a} and C_{3a} replace C_2 and C_3, and $\chi^*(\rho)$ is a new function. Defining $p^* = (C_2^* - C_4^*)/C_3^*$, $q^* = C_1^*/C_3^*$,

$$\chi^*(\rho) = 2\alpha^*\beta^*\left(\alpha^{*2} + \beta^{*2}\right)\frac{\cosh 2\alpha^*\rho + \cos 2\beta^*\rho}{\beta^* \sinh 2\alpha^*\rho - \alpha^* \sin 2\beta^*\rho} \qquad \text{for } \frac{4q^*}{p^{*2}} > 1 \tag{23}$$

$$\chi^*(\rho) = \alpha^*\beta^*\left(\beta^{*2} - \alpha^{*2}\right)\frac{1}{\beta^* \tanh \alpha^*\rho - \alpha^* \tanh \beta^*\rho} \qquad \text{for } \frac{4q^*}{p^{*2}} < 1 \tag{24}$$

where for $4q^*/p^{*2} > 1$

$$\alpha^* = \frac{1}{2}\sqrt{2\sqrt{q^*} - p^*} \qquad \text{and} \qquad \beta^* = \frac{1}{2}\sqrt{2\sqrt{q^*} + p^*} \tag{25}$$

and for $4q^*/p^{*2} < 1$

$$\alpha^* = \sqrt{-\frac{p^*}{2} + \sqrt{\frac{p^{*2}}{4} - q^*}} \qquad \text{and} \qquad \beta^* = \sqrt{-\frac{p^*}{2} - \sqrt{\frac{p^{*2}}{4} - q^*}} \tag{26}$$

As with $[0_n/90_m]_s$ laminates, the expression for the compliance of $[90_n/0_m]_s$ laminates (Eq. (21)) has no adjustable parameters and is applicable to any distribution of crack spacings (not just periodic arrays of cracks). We do not yet have experimental data that can be used to compare predictions to observations.

The total strain energy in the N crack intervals and the longitudinal thermal expansion coefficients are given by expressions identical to the $[0_n/90_m]_s$ laminates (see Eqs. (14) and (15)). A difference between $[90_n/0_m]_s$ and $[0_n/90_m]_s$ laminates occurs because the expressions for compliance, C, that must be used with Eqs. (14) and (15), differ. Finally, combining all expressions, we can derive an expression for the energy release rate due to the formation of additional microcracks

$$G_m = \left(\frac{E_T}{E_c}\sigma_0 - \frac{\Delta\alpha\Delta T}{C_1}\right)^2 C_{3a}t_1 \frac{d}{dD}\left(D\langle\chi_a(\rho)\rangle\right) \tag{27}$$

where $\langle\chi_a(\rho)\rangle$ is the average value of $\chi_a(\rho)$ over the N unit cells of damage.

If we assume that the formation of microcracks is governed by a critical energy release rate or micro-cracking fracture toughness, G_{mc}, we can use Eq. (27) to predict the initiation and the increase in crack density in $[90_n/0_m]_s$ laminates. To use Eq. (27), we must evaluate the density derivative of $D\langle\chi_a(\rho)\rangle$. If we consider the cracking process in Fig. 3B, which perpetuates the staggered arrangement of microcracks, we can evaluate the derivative by the methods used for $[0_n/90_m]_s$ laminates [19,20]. The result is

$$G_m = \frac{1}{2}\left(\frac{E_T}{E_c}\sigma_0 - \frac{\Delta\alpha\Delta T}{C_1}\right)^2 C_{3a}t_1\left(3\chi_a(\rho/3) - \chi_a(\rho)\right) \tag{28}$$

Given a value of the fracture toughness of a material system, G_{mc}, we can solve Eq. (28) for applied stress, σ_0, and predict the crack density as a function of applied stress. Our first experiments have been with Hercules 3501-6/AS4 carbon fiber/epoxy laminates; the results for a $[90_2/0/90_2]_T$ laminate are given in Fig. 5. To be useful, G_{mc} should be a material constant that is independent of stacking sequence. We thus fit the $[90_2/0/90_2]_T$ laminate results using the G_{mc} of 240 J/m^2 found during experiments on $[0_n/90_m]_s$ laminates [20]. The results in Fig. 5 show that Eq. (28) fits the experimental results at high crack density and at zero crack density (microcrack initiation) but shows some deviations at crack densities between 0.0 and 0.4 cracks/mm. The cause of the deviations will require more analysis. We speculate, however, that it is related to the discrete evaluation of the density derivative of $D\langle\chi_a(\rho)\rangle$ inherent in Eq. (28). When the crack

density is low and the microcracks are far apart, the local stress maxima located at $\pm\rho/3$ become diffuse and move away from $\pm\rho/3$ towards $\pm\rho/2$. In other words, it is only at high crack densities that the distribution of the stresses causes cracks to form at $\pm\rho/3$, that damage is driven towards a staggered cracking pattern, and that Eq. (28) gives the true energy release rate. At low crack densities, the cracks will be more random and the expression for energy release rate needs to be modified. Experiments which measure the crack patterns at low crack densities can be used to confirm this speculation and to suggest ways to modify Eq. (28).

Although much more difficult than previous analyses, a closed-form variational mechanics analysis of $[90_n/0_m]_s$ laminates has been obtained. Literature results concentrate of $[0_n/90_m]_s$ laminates to the near exclusion of $[90_n/0_m]_s$ laminates. Clearly more experimental results for $[90_n/0_m]_s$ are desirable. It is our expectation that the variational mechanics analysis will provide the tools necessary for a quantitative understanding of those results.

MICROCRACKING IN $[\pm\theta/90_m]_s$ AND IN $[90_n/\pm\theta]_s$ LAMINATES

The results in the previous two sections can readily be adapted to handle problems of microcracking in 90° plies supported by any orthotropic sublaminate. One simple example is microcracking in $[\pm\theta/90_m]_s$ and in $[90_n/\pm\theta]_s$. In these laminates, θ should be relatively small ($e.g.$ $\theta \leq 45$) or else microcracking of the 90° plies may not be the dominant failure mode. The adaptation of the variational mechanics analysis consists merely of adjusting the constants C_1 to C_4, C_{2a}, C_{3a}, and C_1^* to C_4^*. We note that each of these constants, defined in Eqs. (8) and (19), is the sum of two terms. In all cases, the first term results from the 90° plies and the second term results from the 0° plies. To construct a solution for laminates in which the 0° plies are replaced by a $[\pm\theta]$ sublaminate, we merely replace the mechanical properties of the 0° plies in each second term with those of the $[\pm\theta]$ sublaminate.

DELAMINATIONS EMANATING FROM THE TIPS OF MICROCRACKS

All variational mechanics analyses of cross-ply and related laminates can be extended to account for delaminations emanating from the tips of existing microcracks. We illustrate the delamination analysis using $[0_n/90_m]_s$ laminates. Figure 6 shows the region between two microcracks separated by a distance $2a$ having delaminations of length d_1 and d_2 emanating from the top and bottom microcracks and propagating into the region between the two microcracks.

We consider the right half of the symmetric laminate in Fig. 6. We split the area between the two existing microcracks into three regions. Region I is the region within the top delamination or the region from $x = a - d_1$ to $x = a$. Region II is the region between the tips of the delaminations or the region from $x = -a + d_2$ to $x = a - d_1$. Region III is the region within the bottom delamination or the region from $x = -a$ to $x = -a + d_2$. Within each region we divide the right half of the laminate into two layers. Layer 1 is the 90° ply group and layer 2 in the 0° ply group.

We begin with the stresses in the 90° plies in regions I and III. By symmetry, the shear stress at the sample middle must be zero $(\sigma_{xz}^{(1)}(0) = 0)$. Because of the requirement for stress free surfaces on the delamination crack face, the shear stress and the normal stress at the right edge of the 90° plies must also be zero $(\sigma_{xz}^{(1)}(1) = 0$ and $\sigma_{zz}^{(1)}(1) = 0)$. From these boundary conditions and the form of the stresses in Eqs. (1)-(3) which assume that the normal stress $\sigma_{xx}^{(i)}$ is a function of x only, the stresses in regions I and III are uniquely determined to be

$$
\begin{aligned}
\sigma_{xx}^{(1)} &= 0 & \sigma_{xx}^{(2)} &= \frac{1+\lambda}{\lambda}\sigma_0 \\
\sigma_{xz}^{(1)} &= \sigma_{zz}^{(1)} = 0 & \sigma_{xz}^{(2)} &= \sigma_{zz}^{(2)} = 0
\end{aligned}
\tag{29}
$$

The boundary conditions in region II are unaffected by the length or even the presence of the delaminations. With or without the delaminations, the x direction tensile stress and the shear stress are both zero at the top and bottom of region II. The stresses in region II are therefore identical to the stresses calculated in Ref. [19] except that the crack spacing needs to be adjusted. We introduce the dimensionless quantity

$$
\delta = \frac{d_1 + d_2}{2t_1}
\tag{30}
$$

The stresses in region II are identical to the stresses calculated in Ref. [19] for two microcracks whose spacing is characterized by $\rho - \delta$.

With the stresses completely determined, we can follow procedures similar to those in Ref. [19] and evaluate properties of microcracked and delaminated cross-ply laminates. Consider a sample with N unit cells of damage characterized by crack spacings $\rho_1, \rho_2, \ldots, \rho_N$ and by extents of delamination within each crack interval of $\delta_1, \delta_2, \ldots, \delta_N$. The sample compliance is

$$C = \frac{L-d}{L}\left(C_0 + \frac{2t_1 C_3 L E_T^2}{B^2 W E_c^2}\frac{\sum \chi(\rho_i - \delta_i)}{\sum(\rho_i - \delta_i)}\right) + \frac{d}{L}\left(\frac{1+\lambda}{\lambda}\frac{L}{BE_A W}\right) \tag{31}$$

where $d = \sum_{i=1}^{N} 2t_1 \delta_i$ is the total sample delamination length. Although we have no experimental evidence to verify Eq. (31), its limiting values are appropriate. In the limit of no delaminations, or $d = 0$, Eq. (31) reduces to Eq. (9). In the limit of complete delamination, or $d = L$, the sample compliance reduces to

$$C_\infty = \frac{1+\lambda}{\lambda}\frac{L}{BE_A W} \tag{32}$$

This is the compliance for a sample in which the 90° plies carry no load. In terms of compliance, the total strain energy is found to be

$$U = \left(\frac{\sigma_0^2}{2E_c} + \frac{t_1 \Delta\alpha^2 \Delta T^2}{C_1 B}\right)(L-d)BW + \frac{\sigma_0^2}{2E_A}\frac{1+\lambda}{\lambda}dBW$$
$$+ \left(C - C_0 - \frac{d}{L}(C_\infty - C_0)\right)\frac{B^2 W^2 E_c^2}{2E_T^2}\left(\frac{E_T^2}{E_c^2}\sigma_0^2 - \frac{\Delta\alpha^2 \Delta T^2}{C_1^2}\right) \tag{33}$$

and the thermal expansion coefficient is found to be

$$\alpha_L = \alpha_L^0 - \frac{d}{L}\frac{\Delta\alpha}{\lambda E_A C_1} - \frac{\Delta\alpha}{C_1 C_0 E_T}\left(C - C_0 - \frac{d}{L}(C_\infty - C_0)\right) \tag{34}$$

The above two-dimensional analysis can immediately be used to find the energy release rate for the growth of a through-the-thickness delamination — G_d. The energy release rate is

$$G_d = -\left.\frac{\partial U}{\partial A}\right|_{const.disp.} = -\frac{1}{2W}\left.\frac{\partial U}{\partial d}\right|_{const.disp.} \tag{35}$$

where A is total delamination area which is equal to $2dW$. We differentiate Eq. (33) realizing that σ_0 and C will depend on d. The result after much simplification (details can be found in Ref. [20]) is

$$G_d = \left(\frac{E_T}{E_c}\sigma_0 - \frac{\Delta\alpha\Delta T}{C_1}\right)^2 C_3 t_1 Y_D(\vec{\rho}, \vec{\delta}) \tag{36}$$

where the function $Y_D(\vec{\rho}, \vec{\delta})$ depends on $\vec{\rho} = (\rho_1, \rho_2, \ldots, \rho_N)$ and on $\vec{\delta} = (\delta_1, \delta_2, \ldots, \delta_N)$. It is given explicitly by

$$Y_D(\vec{\rho}, \vec{\delta}) = \frac{B^2 W E_c^2}{4E_T^2 C_3 t_1}\left(\frac{C_\infty - C}{L-d}\right) + \left(\frac{L-d}{2}\right)\frac{\partial}{\partial d}\frac{\sum \chi(\rho_i - \delta_i)}{\sum(\rho_i - \delta_i)} \tag{37}$$

Imagine a sample with N crack intervals characterized by dimensionless crack spacings and delamination lengths defined by the vectors $\vec{\rho}$ and $\vec{\delta}$. Imagine further some delamination growth confined to the kth crack interval. The $Y_D(\vec{\rho}, \vec{\delta})$ function for this delamination growth simplifies to [20]

$$Y_D(\vec{\rho}, \vec{\delta}) = \frac{1}{2}(\chi'(0) - \chi'(\rho_k - \delta_k)) \tag{38}$$

The differentiation of $\chi(\rho)$ is with respect to the variable ρ.

504

If we assume that delamination will propagate when $G_d > G_{dc}$ where G_{dc} is a critical energy release rate or *interlaminar* fracture toughness, we can use Eq. (36) to predict the initiation and growth of micro-crack induced through-the-width delaminations. One possible problem of this approach is that it uses total energy release rate instead of partitioning it into the various modes — mode I, mode II, and mode III. We suggests that the assumed x-direction propagation of a through-the-width delamination will be mostly mode II deformation. The distinction between using total energy release rate and the mode II part of the energy release rate will therefore be minor. Experimental results are required to determine the adequacy of using total energy release rate as a failure criterion. For the purpose of this discussion, we assume that the total energy release rate failure criterion is valid.

We can use the delamination analysis to discuss competition between microcracking and delamination. The first form of damage in cross-ply laminates is always microcracking. Once the first microcrack has formed, we can ask if a delamination will initiate at that microcrack or if instead another microcrack will form. Comparing the energy release rate for microcracking (Eq. (17)) to the energy release rate for delamination (Eq. (36)), the predicted failure mode will depend on the values of G_{mc} and G_{dc} and on the relative magnitudes of $2\chi(\rho/2) - \chi(\rho)$ and $\frac{1}{2}(\chi'(0) - \chi'(\rho))$. Assuming G_{mc} and G_{dc} are the same (they both represent crack growth through the matrix, albeit possibly by different fracture modes — mode I vs. mode II), the predicted failure mode can be determined by plotting the latter two quantities. Figure 7 plots $2\chi(\rho/2) - \chi(\rho)$ and $\frac{1}{2}(\chi'(0) - \chi'(\rho))$ for a typical $[0/90_2]_s$ laminate. The conclusions that can be drawn from this and other similar plots are as follows:

1. At low crack densities, microcracking is preferred. At some critical density, the energy release rate for delamination will surpass the energy release rate for microcracking and delaminations will be expected to initiate at the tips of the microcracks. Once delaminations begin, microcracking will cease and the delaminations will grow.

2. The critical density depends on the laminate structure. For a fixed number of 0° plies, the more 90° plies there are, the lower will be the crack density required to get delamination. For a fixed ratio of 0° to 90° plies, the more plies there are, the lower will be the crack density required to get delamination.

3. If the relative toughnesses for microcracking and delamination are different because of material properties of because of different deformation modes, the critical density for initiation delamination will change. For example, as the delamination fracture toughness gets lower than the microcracking fracture toughness, the critical crack density to initiate delamination will get lower. In the limit of relatively low delamination fracture toughness, delamination will begin after the first microcrack.

When delamination is not through-the-thickness, the problem is no longer two-dimensional and requires a three-dimensional analysis. Although a complete three-dimensional variational mechanics analysis seems intractable, it appears possible to construct a quasi-three-dimensional analysis based on the two-dimensional analysis and a lumped spring model of a laminate containing an arbitrary profile of delamination growth. This problem will be considered in a future publication.

ACKNOWLEDGMENTS

REFERENCES

1. H. T. Hahn and S. W. Tsai, *J. Comp. Mat.*, **8**, 288 (1974).
2. K. W. Garret and J. E. Bailey, *J. Comp. Mat.*, **12**, 157 (1977).
3. A. L. Highsmith and K. L. Reifsnider, *ASTM STP*, **775**, 103 (1982).
4. A. Parvizi, K. W. Garrett, and J. E. Bailey, *J. Mat. Sci.*, **12**, 195 (1978).
5. D. L. Flaggs and M. H. Kural, *J. Comp. Mat.*, **16**, 103 (1982).
6. M. G. Bader, J. E. Bailey, P. T. Curtis, and A. Parvizi , *Proc. 3rd Int'l Conf. on Mech. Behavior of Materials*, **3**, 227 (1979).
7. J. E. Bailey, P. T. Curtis, and A. Parvizi, *Proc. Roy. Soc. London*, **A366**, 599 (1979).

8. S. E. Groves, C. E. Harris, A. L. Highsmith, and R. G. Norwell, *Exp. Mech.*, 73 (March, 1987).

9. L. Boniface, P. A. Smith, S. L. Ogin, and M. G. Bader, *Proc. 6th Int'l Conf. on Composite Materials*, **3**, 156 (1987).

10. L. Boniface and S. L. Ogin, *J. Comp. Mat.*, **23**, 735 (1989).

11. C. T. Herakovich and M. W. Hyer, *Eng. Fract. Mech.*, **25**, 779 (1986).

12. D. S. Adams and C. T. Herakovich, *J. Thermal Stresses*, **7**, 91 (1984).

13. D. E. Bowles, *J. Comp. Mat.*, **17**, 173 (1984).

14. P. W. Manders, T. W. Chou, F. R. Jones, and J. W. Rock, *J. Mat. Sci.*, **18**, 2876 (1983).

15. D. L. Flaggs, *J. Comp. Mat*, **19**, 29 (1985).

16. Z. Hashin, *Mechanics of Materials*, **4**, 121 (1985).

17. Z. Hashin, *Eng. Fract. Mech.*, **25**, 771 (1986).

18. Z. Hashin, *Comp. Sci. & Tech.*, **31**, 247 (1988).

19. J. A. Nairn, *J. Comp.Mat.*, **23**, 1106 (1989).

20. J. A. Nairn, Quarterly Report for NASA Contract NAS1-18833, June 1, 1990 (Note: report contains preprint of S. Liu and J. A. Nairn, *J. Comp. Mat.*, submitted, a paper that describes the $[0_n/90_m]_s$ experiments).
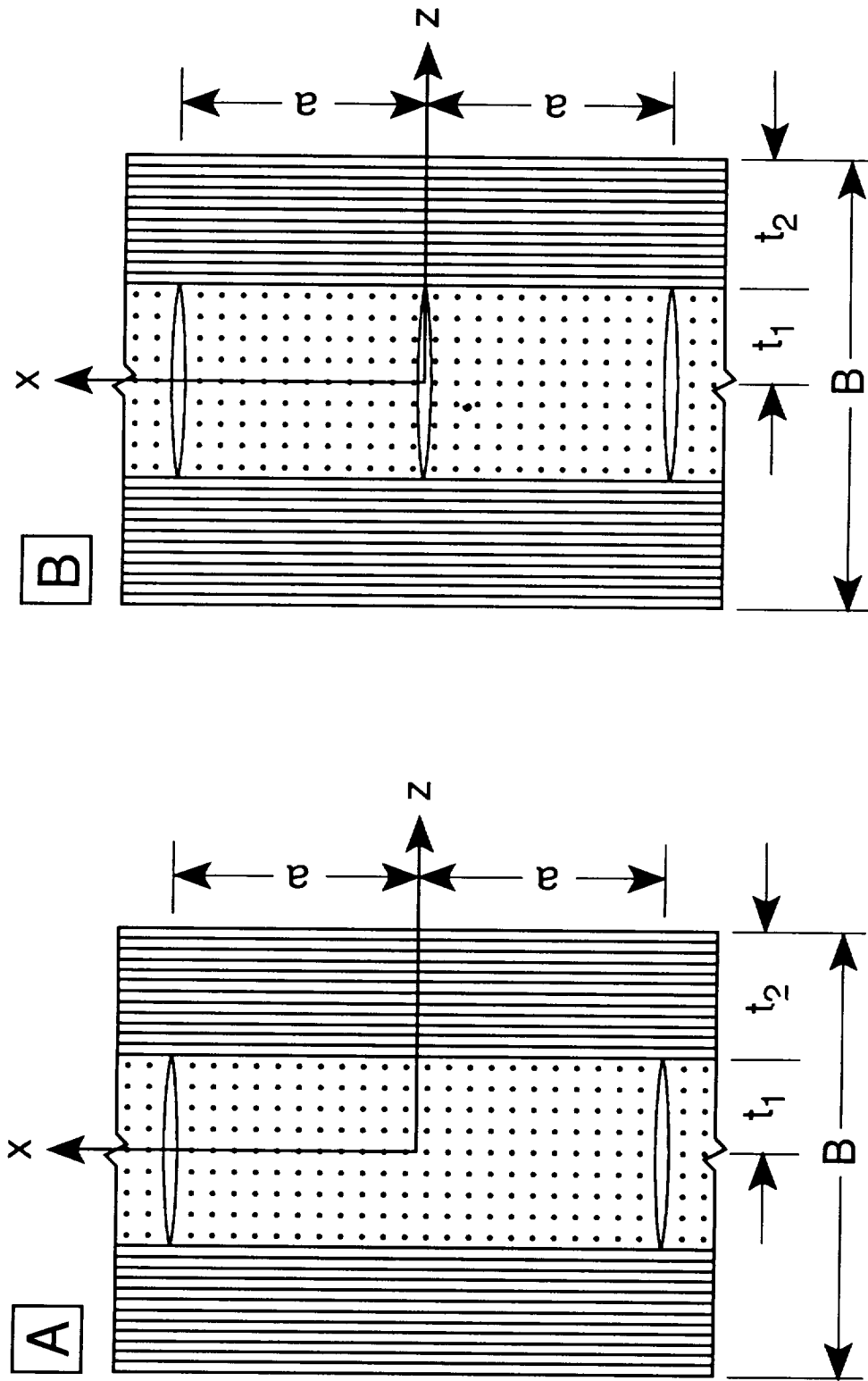
Figure 1: Edge view of a $[0_n/90_m]_s$ cross-ply laminate with microcracks. A: Two microcracks in the 90° plies. B: The formation of a new microcrack midway between to two existing microcracks.
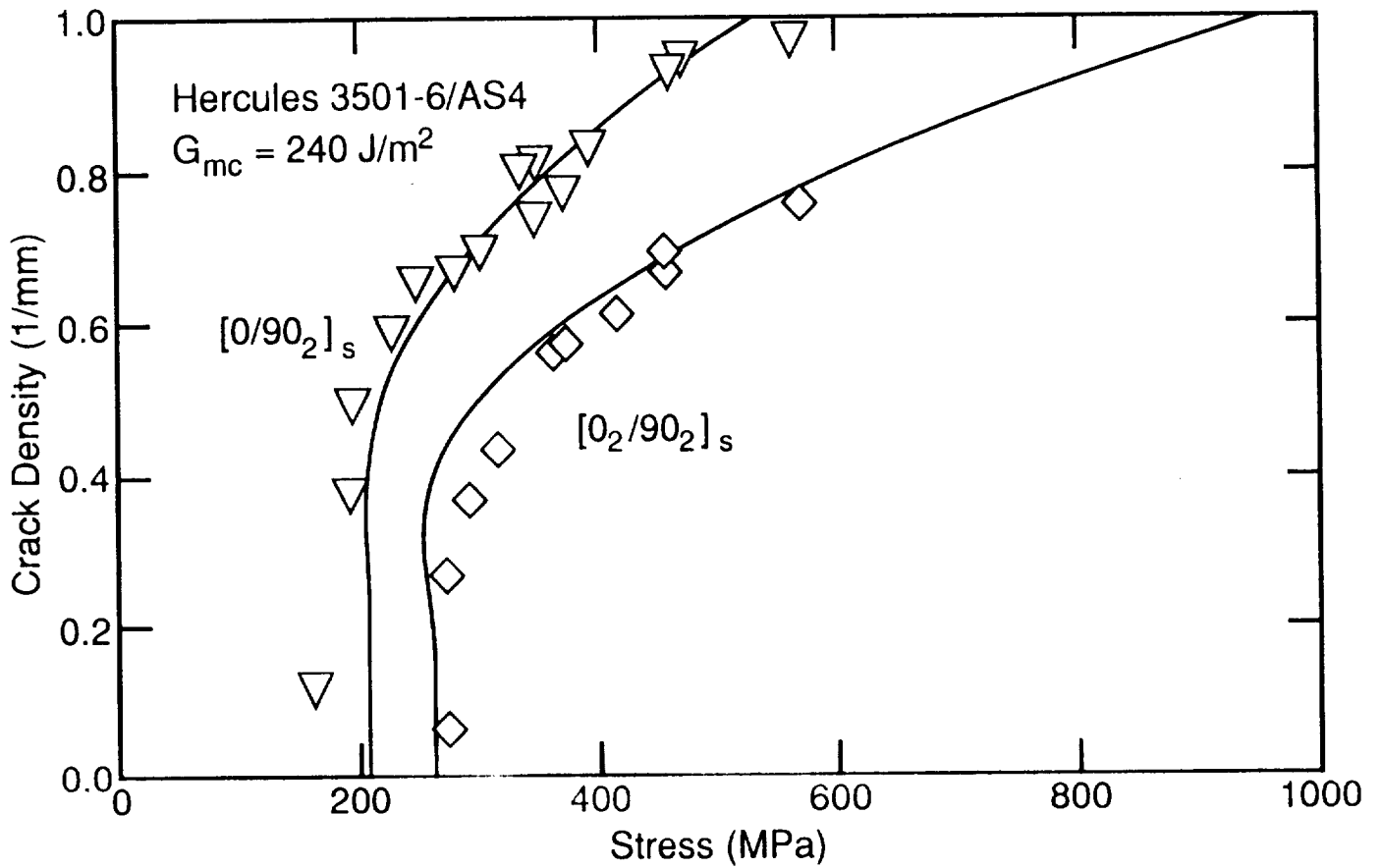
507

Figure 2: The microcrack density as a function of applied load in Hercules 3501-6/AS4 carbon fiber/epoxy cross-ply laminates. The symbols are experimental data points and the smooth lines are best fits using G_{mc} of 240 J/m^2.
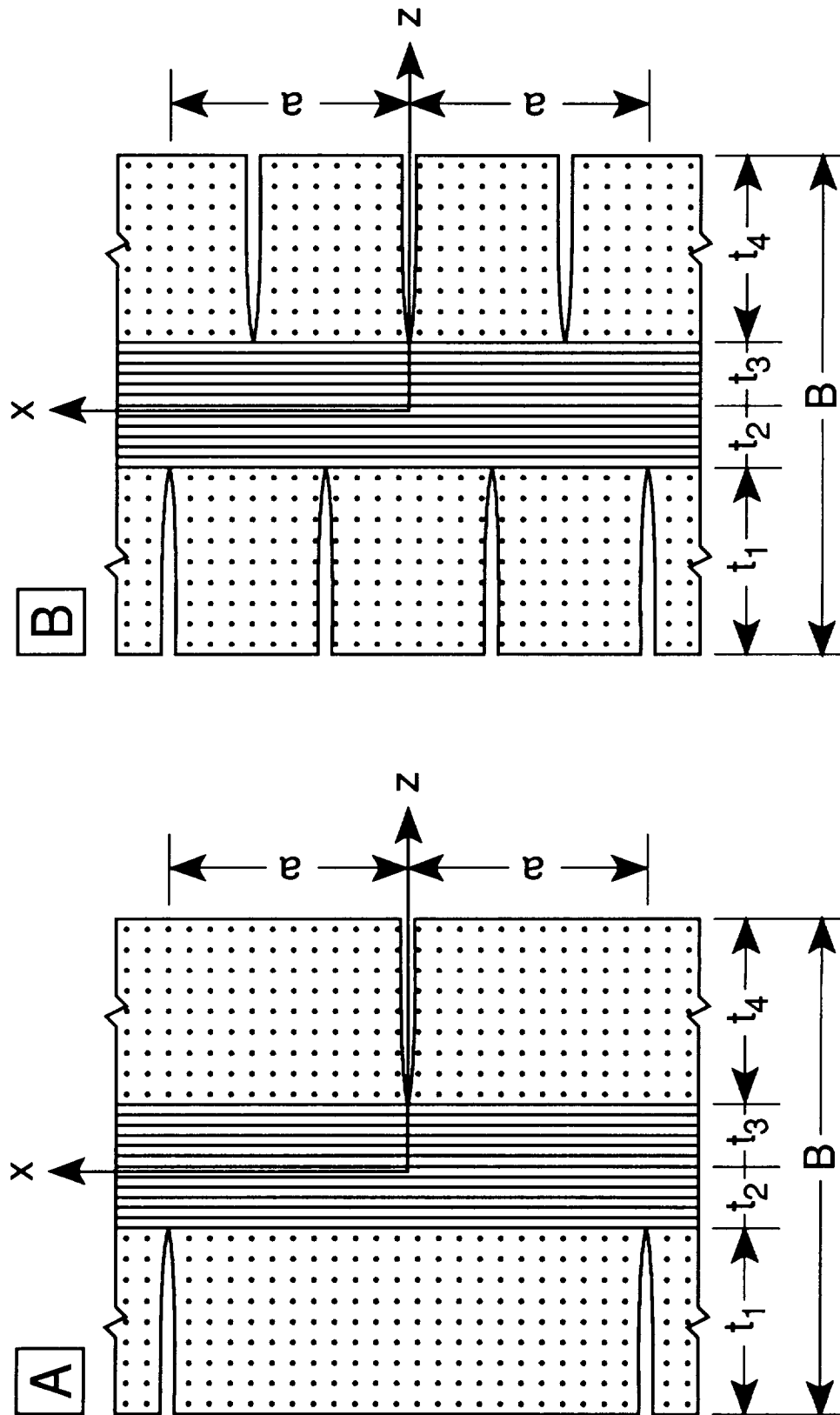
Figure 3: Edge view of a $[90_n/0_m]_s$ cross-ply laminate with microcracks. A: Staggered microcracks in the 90° plies. B: The formation of a new microcracks $\frac{1}{3}$ and $\frac{2}{3}$ of the way between existing microcracks.
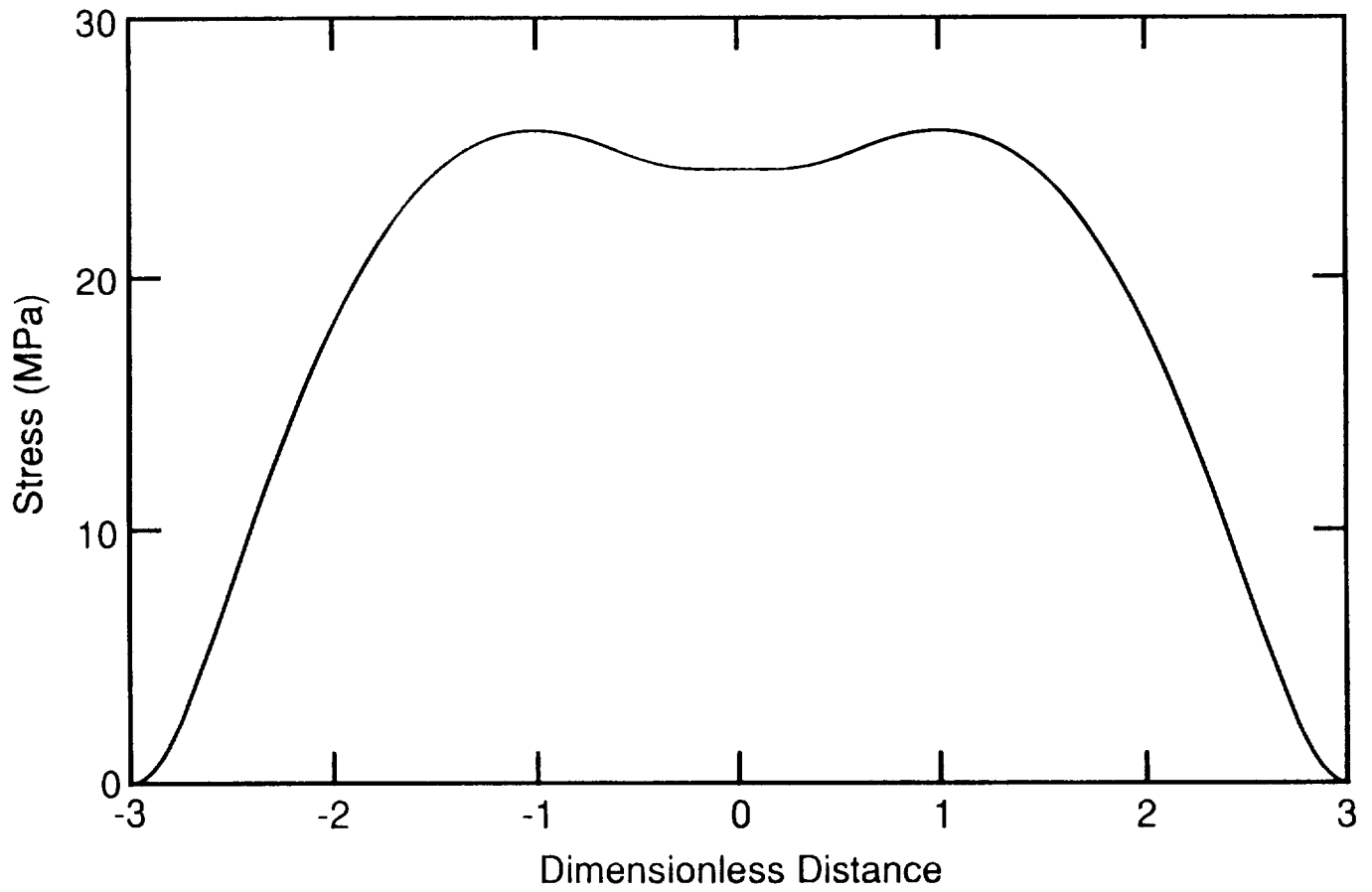
Figure 4: The x direction tensile stress in the 90° ply in a $[90_2/0]_s$ carbon fiber/epoxy laminate ($\sigma_{xx}^{(1)}$). This ply has microcracks located at $\rho = \pm 3$.
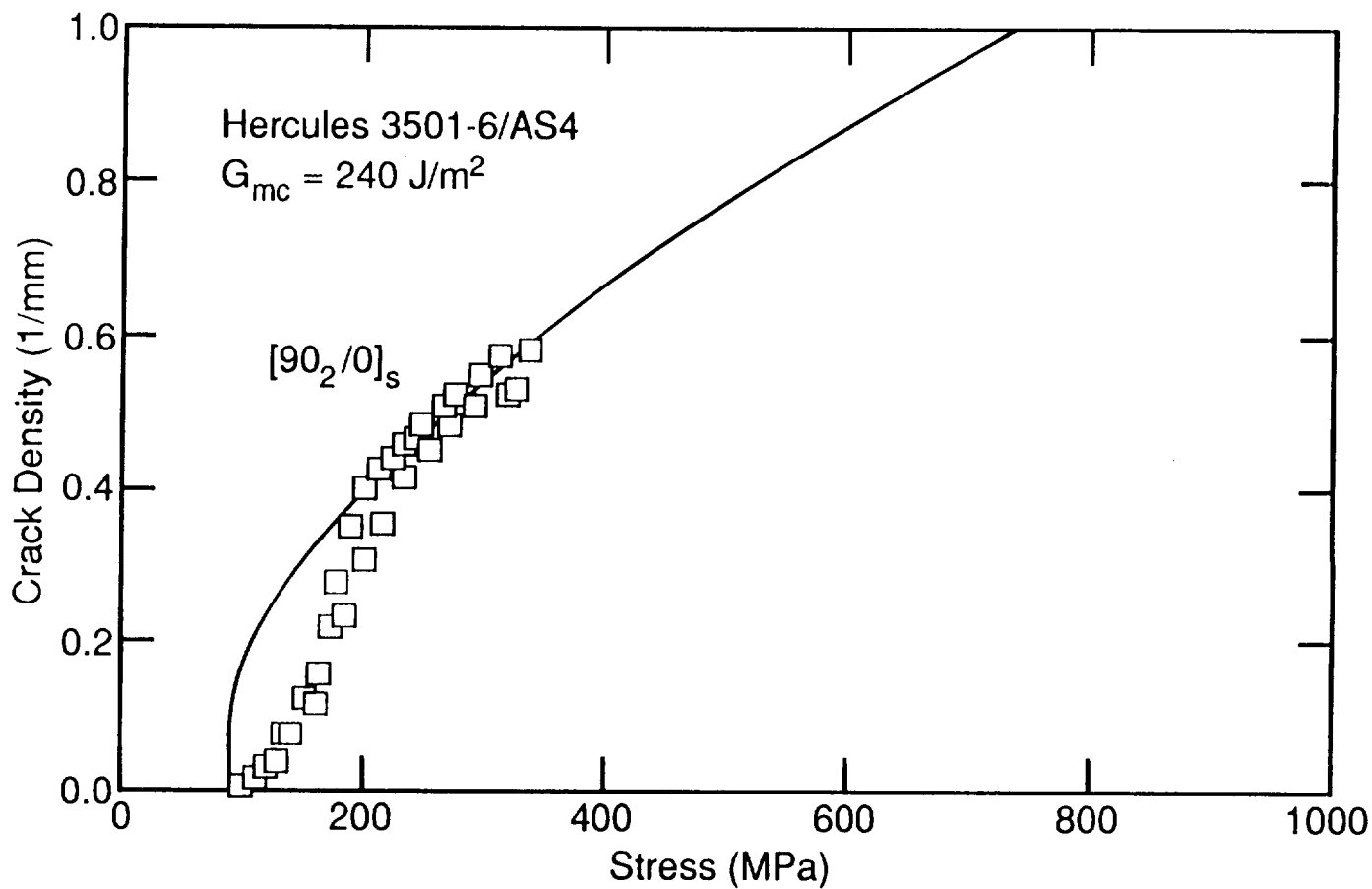
Figure 5: The microcrack density as a function of applied load in a Hercules 3501-6/AS4 carbon fiber/epoxy $[90_2/0]_s$ laminate. The symbols are experimental data points and the smooth line is calculated using G_{mc} of 240 J/m^2.
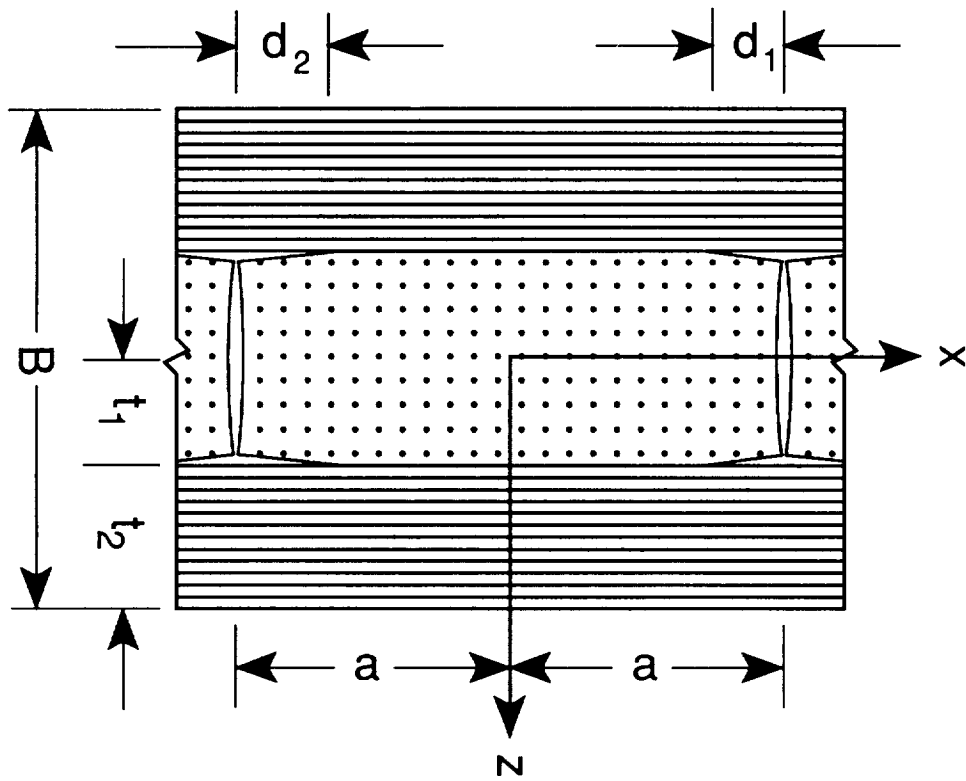
Figure 6: Edge view of a $[0_n/90_m]_s$ cross-ply laminate with microcracks and delaminations emanating from the tips of those microcracks.
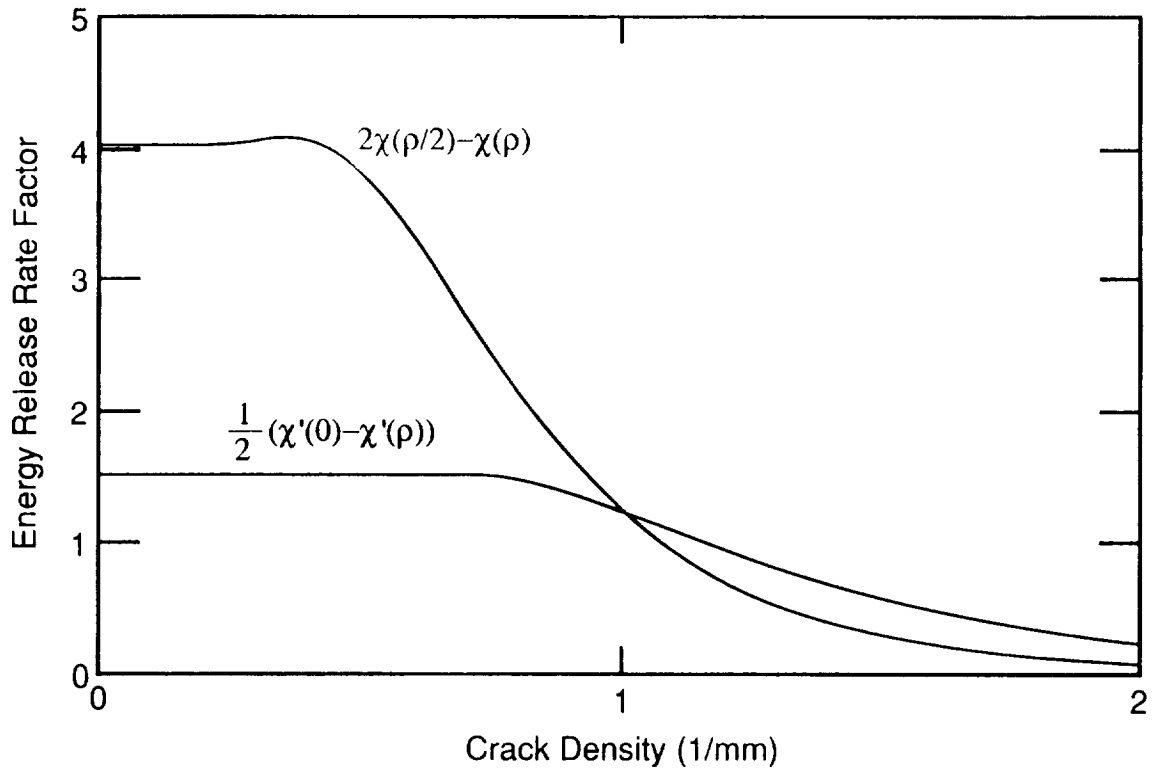

Figure 7: The energy release rate factor for microcracking $[\,2\chi(\rho/2) - \chi(\rho)]$ and for delamination $[\frac{1}{2}(\chi'(0) - \chi'(\rho))]$ as a function of crack density.